Journal of Casting & Materials Engineering Vol. 10 No. 1 (2026) 10–15
https://doi.org/10.7494/jcme.2026.10.1.10

# Determination of the Heat Transfer Coefficient in the Isothermal Quenching Process of ADI Cast Iron Cooled with Water Mist

**Andriy Burbelko[a], Piotr Stręk[a*]**

[a] AGH University of Krakow, Faculty of Foundry Engineering, 23 Reymonta St., 30-059 Krakow, Poland

**e-mail: piotr@ledavi.com*



Received: 12 March 2026/Accepted: 19 March 2026/Published online: 31 March 2026.
This article is published with open access at AGH University of Science and Technology Journals.

**Abstract**

Isothermal quenching of austempering cast iron (ADI) castings requires that, after austenitization the casting must be rapidly cooled to the temperature of isothermal austenite decomposition. The cooling rate throughout the entire volume of the heat-treated product must be high enough to prevent pearlitic transformation. At the same time, the temperature of the cooled surface must not decrease below the martensitic transformation start temperature $M_s$. The cooling rate of the casting surface is determined by factors such as the temperature difference between the surface of the cooled casting and the cooling medium, the thermal conductivity of cast iron, the heat transfer coefficient, and the wall thickness of the treated casting. In the case of cooling with water mist, the heat transfer coefficient depends on the temperature of the cooled surface. To control the cooling process of castings using water mist, information about this relationship for the temperature range of 200–800°C is needed. Available scientific publications on this subject contain contradictory data.

Therefore, a measuring station was built with the ability to set the temperature of the cooled surface. The station includes a measuring system that allows the measurement of the heat flux flowing from the heating element into the environment. The result of the research is the measurement of the relationship between the temperature of the cooled surface and the heat transfer coefficient. The values obtained will be used in the future to build a numerical model of ADI castings heat treatment. This work may contribute to the future replacement of salt baths (currently used for fast cooling and austempering) with water mist spraying. In this case, the low-temperature operation of austenite decomposition can be performed without the use of salt a bath.

**Keywords:**

austempered ductile iron, austempering, water mist, heat transfer coefficient, heat treatment

## 1. INTRODUCTION

Article [1] presents the theoretical possibilities of controlling the cooling rate in the heat treatment of cast iron using water mist spraying. The advantages of using water mist include: economics, the high specific heat of the phase transition of water droplet evaporation, and environmental friendliness. These advantages have been recognized by numerous researchers, including [2] and [3]. However, one challenge when applying this method is achieving precise control of heat transfer to prevent the $M_s$ temperature from reaching the surface layer of the cooled casting. There are many publications on the measurement of the heat transfer coefficient during the spray cooling of metal surfaces with water mist. In these studies the coefficient was determined using the conduction equation under either steady state [4–7] or unsteady state [8–16] heat flow conditions.

Unfortunately, the research methods and results presented in the literature do not cover the temperature range of interest to us, including ADI isothermal hardening and a material such as cast iron. Therefore, a research method has been designed and presented in this article to fill the research gap not yet represented in the literature. It should be noted that many factors influence the value of the determined coefficient. These factors include the size of the spray droplets and their velocity and the water flow rate. The influence of these parameters, among others, have been investigated and described in publication [17]. The effects of the type of cooled material and the roughness of the cooled surface are described in [18, 19]. At this stage of the research the above factors were assumed to be constant. The examined dependence of the heat transfer coefficient on temperature will be used to create a numerical model that would describe the phenomena occurring during the cooling of austempered ductile iron. The proposed measurement method is based on established heat transfer conditions.

## 2. TEST SETUP

The measurement system is shown schematically in Figure 1. The plate (2) made of ductile iron is cooled on one side by water spray (3) and heated on the other side (4). A type K thermocouple (1) is welded to the heated side of the plate. A diagram of the plate and the location of the thermocouple weld is shown in Figure 2. The cooled surface of the plate has not been machined and corresponds to the surface of the casting after it has been removed from the mold. The temperature is measured by a Keysight 34465A multimeter (7), while the measurement is set by a trigger controller (8). The individual parts of the heating element are designed in such a way that heat is released in the part located directly under the measuring plate (Figs. 3 and 4). This reduces heat loss. In addition, a layer of thermally conductive adhesive is used thatimproves heat transfer between the heating element and the test plate. The heating element is insulated with ceramic tiles to limit heat transfer to the environment other than through the measuring plate. The heating element is connected via a discrete transistor current controller (6) to a power supply with a capacity of 300 A and a voltage of 5 V. The connecting cables for the high-current part have a cross-section of 2×35 mm$^2$. The discrete current and power output controller on the heating element is implemented using parallel-connected MOSFET transistors controlled by integrated gate controllers. The discrete current controller (6) is galvanically isolated from the trigger controller (8) by a fiberoptic link. The Keysight DAQ970A data logger (9) and the appropriate card attached to the logger (Keysight DAQM901A) are used to measure the current and voltage on the heating element. The voltage is measured directly by the data logger, while the current is measured by the LT1000-TI current-voltage converter (5). The voltage generated by the converter is proportional to the current flow in the high-voltage cables supplying the heating element. Measurements taken by the multimeter and recorder are read cyclically using a PC (10). The data is read via an Ethernet connection and processed by proprietary software. The cyclical temperature reading is used by a software-implemented PI (proportional integral) controller to determine the deviation between the set temperature and the temperature read from the thermocouple. The calculated deviation is the basis for calculating the duty cycle of the control pulse that opens the MOSFET transistors in the current controller (6). Data on the desired duty cycle is sent from the computer in digital form to the trigger controller (8).

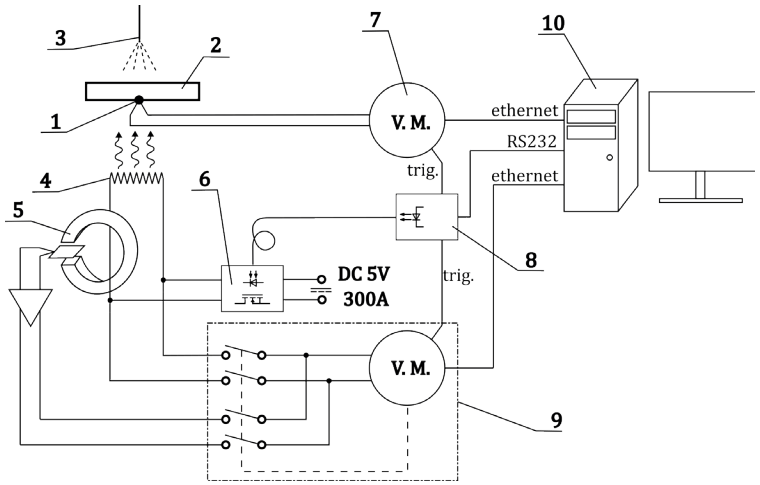


**Fig. 1.** Measurement system diagram: 1 – thermocouple, 2 – measuring plate, 3 – spray nozzle, 4 – heating element, 5 – current voltage converter, 6 – discrete current controller, 7 – multimeter, 8 – measurement trigger controller, 9 – data logger, 10 – PC

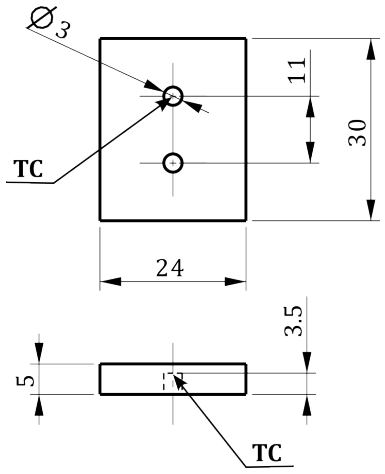


**Fig. 2.** Dimensions of the measuring plate (TC – thermocouple welding point)

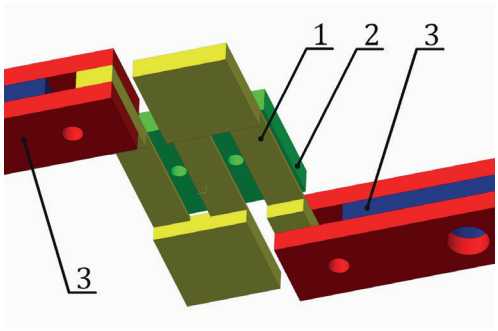


**Fig. 3.** Mutual position of the test plate and the heating element: 1 – heating element, 2 – measuring plate, 3 – power supply terminals

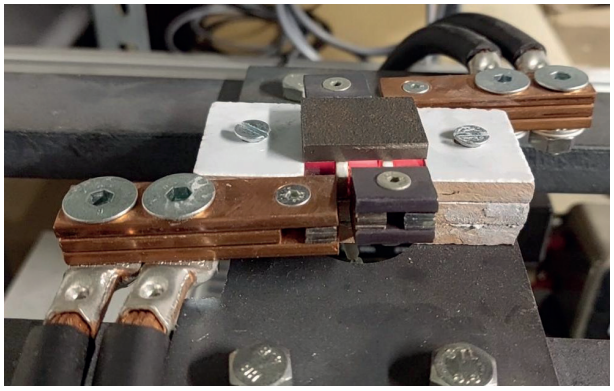

**Fig. 4.** Heating element with ceramic insulation and measuring plate

The hydraulic-air system diagram is shown in Figure 5. The heated measuring plate is cooled using a single-phase full-cone nozzle with a spray angle of 30° (3); manufacturer's symbol: BEX 1/8GS3001.4 V2A. The hydraulic-air system cycle begins with filling the water tank (1) by opening the valve supplying water from the water supply network. The filling is checked by observing the overflow valve. The valve supplying compressed air remains closed at this point. After filling the tank the water supply and overflow valves are closed. In the next step the compressed air tank (2) is filled to a pressure of 8 bar using a compressor (5). Once this pressure is reached the safety switch opens the compressor's power supply. The desired water outlet pressure is set on the pressure reducer (4). To start the measurement the valve supplying air to the water tank is opened, followed by the valve connecting the spray nozzle (3) and the water tank (1).

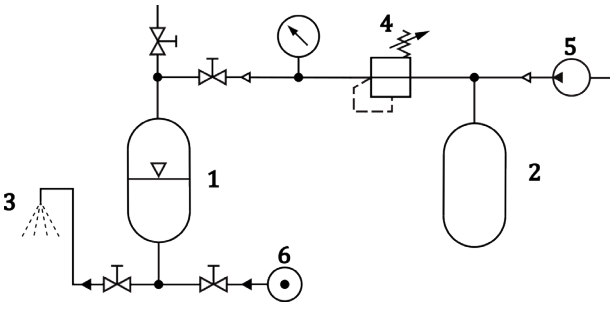


**Fig. 5.** Diagram of the hydraulic-air system of a heat transfer coefficient measurement station: 1 – cooling water tank, 2 – compressed air tank, 3 – spray nozzle, 4 – pressure reducer, 5 – compressor, 6 – service water supply

Figure 6 shows a heated measuring plate made of cast iron cooled by active water-mist spraying. A trough is visible, the task of which is to collect and feed unused water to cool the measuring plate and protect components that not get wet.

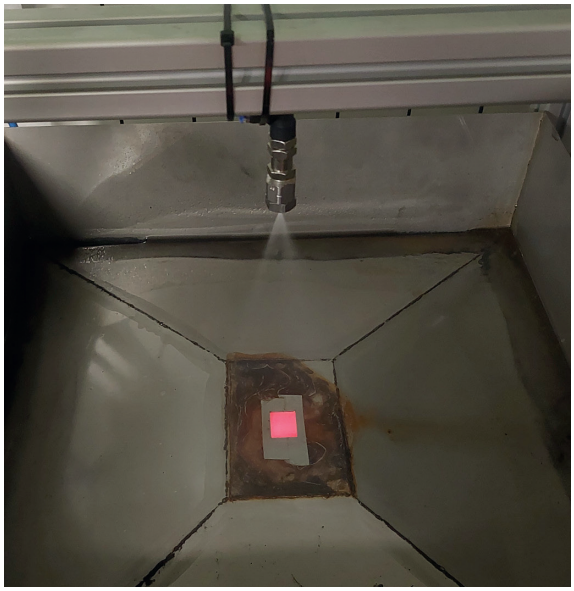

**Fig. 6.** View of the station during the research

## 3. MEASUREMENT CONDITIONS AND RESULTS

In the first step the nozzle capacity was tested. It amounted to 0.55 l/min at a pressure of 3 bar. The distance between the nozzle and the measuring plate is 200 mm. Considering that the spray angle of the nozzle is 30°, the surface area sprayed by the nozzle is $9.022 \cdot 10^{-3}$ m$^2$, while the surface area of the measuring plate onto which the spray falls is 0.024 m × 0.030 m = $0.72 \cdot 10^{-3}$ m$^2$. A test was carried out that showed that the sprayed stream has the same efficiency over the entire sprayed surface (Fig. 7). The test consisted of measuring the height $L$ of the water column in a measuring cup during 1 minute of nozzle operation. The test was carried out at 6 points on the sprayed surface. No deviations in height $L$ were found during the measurement.

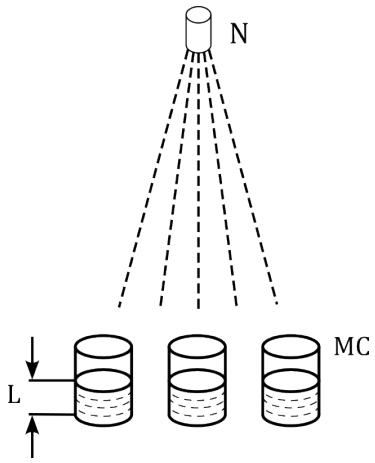


**Fig. 7.** Schematic representation of spray-intensity uniformity measurement, where N – nozzle, MC – measuring cup

Therefore, the $\eta_m$ spray consumption converted to the sprayed tile surface area could be calculated using the following formula:

$$\eta_m = \rho_v \cdot \left( \frac{P_p}{P_c} \right) \quad (1)$$

where:

$\eta_m$ – spray rate converted to the sprayed surface area of the measuring plate, g/s,
$\rho_v$ – nozzle capacity (9.166 g/s),
$P_c$ – total area sprayed by the nozzle ($9.02 \cdot 10^{-3}$ m$^2$),
$P_p$ – the surface area of the tile that was sprayed ($0.72 \cdot 10^{-3}$ m$^2$),

The spray coefficient, converted to the sprayed surface area of the test panel, is: $\eta_m$ = 0.731 g/s

We assumed that all of the water sprayed onto the tile surface would be heated to 100°C and then converted into steam. In our calculations we ignored the specific heat of the water vapor. The total maximum power that could be dissipated from the sprayed tile surface under these assumptions could be calculated using the following formula:

$$P_c = \left[ c_V \cdot (100 - 20) + c_p \right] \cdot \eta_m \quad (2)$$

where:

$P_c$ – theoretical total power that could be dissipated by water mist spray,
$c_V$ – the specific heat of the water (4.184 kJ/(kg·K)),
$c_p$ – the heat of the vaporization of the water (2260 kJ/kg).

After substituting the data we obtained the maximum power that could be dissipated from the surface of the plate at a level of $P_c$ = 1895.9 W, which gave a theoretical heat flux intensity of 2633 kW/m$^2$.

In the second step, thanks to the PI controller, the target temperature value $T_m$, measured by the thermocouple was set (Fig. 8), which, under the designed geometric conditions (Fig. 2), was very close to $T_p$. After the measured temperature stabilized, ten measurements of the heat output $Q_T$ were recorded. All measurement results are presented in Figure 9.

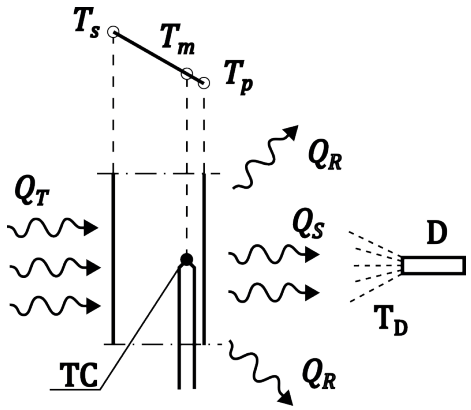


**Fig. 8.** Temperature field and thermocouple (TC) location: $T_s$ – heating element temperature, $T_m$ – thermocouple temperature, $T_p$ – surface temperature, $T_D$ – water mist temperature, $Q_T$ – heat emitted by the heating element, $Q_R$ – heat flux flowing to the environment in a manner other than through the cooled surface of the test plate, $Q_S$ – heat flux dissipated by water mist spray

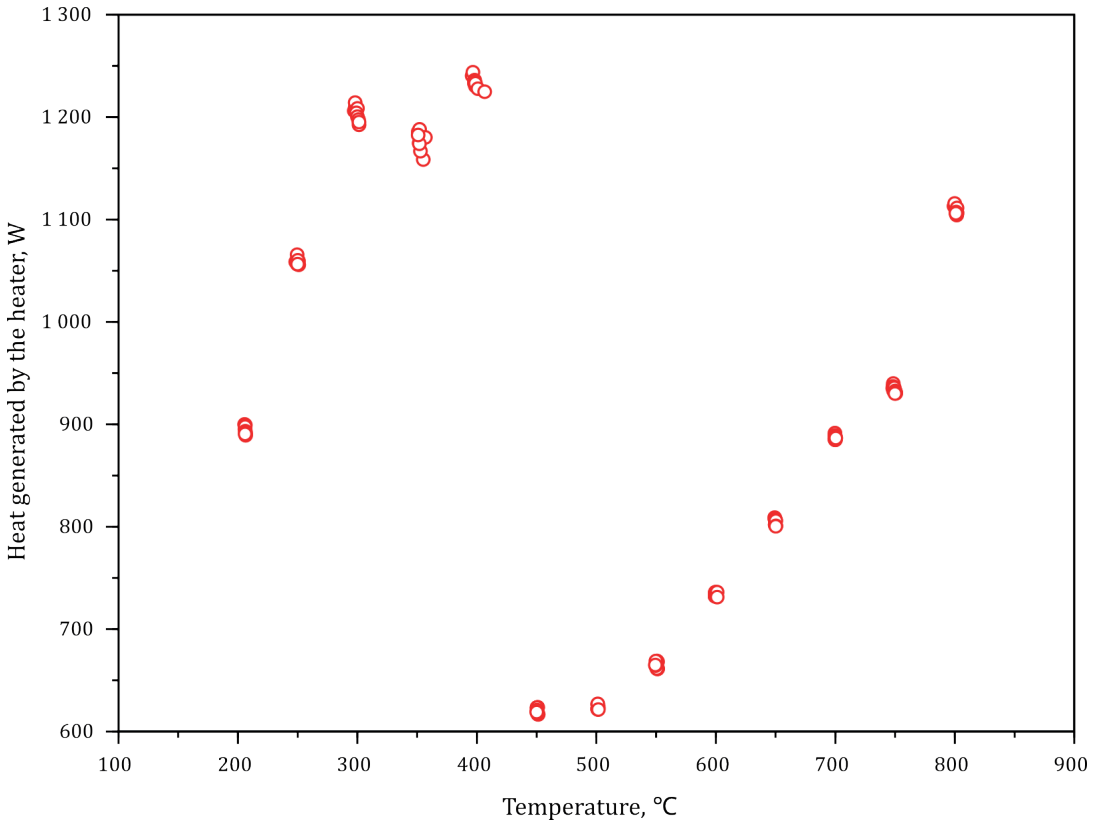


**Fig. 9.** Power dissipated on the heating element as a function of temperature

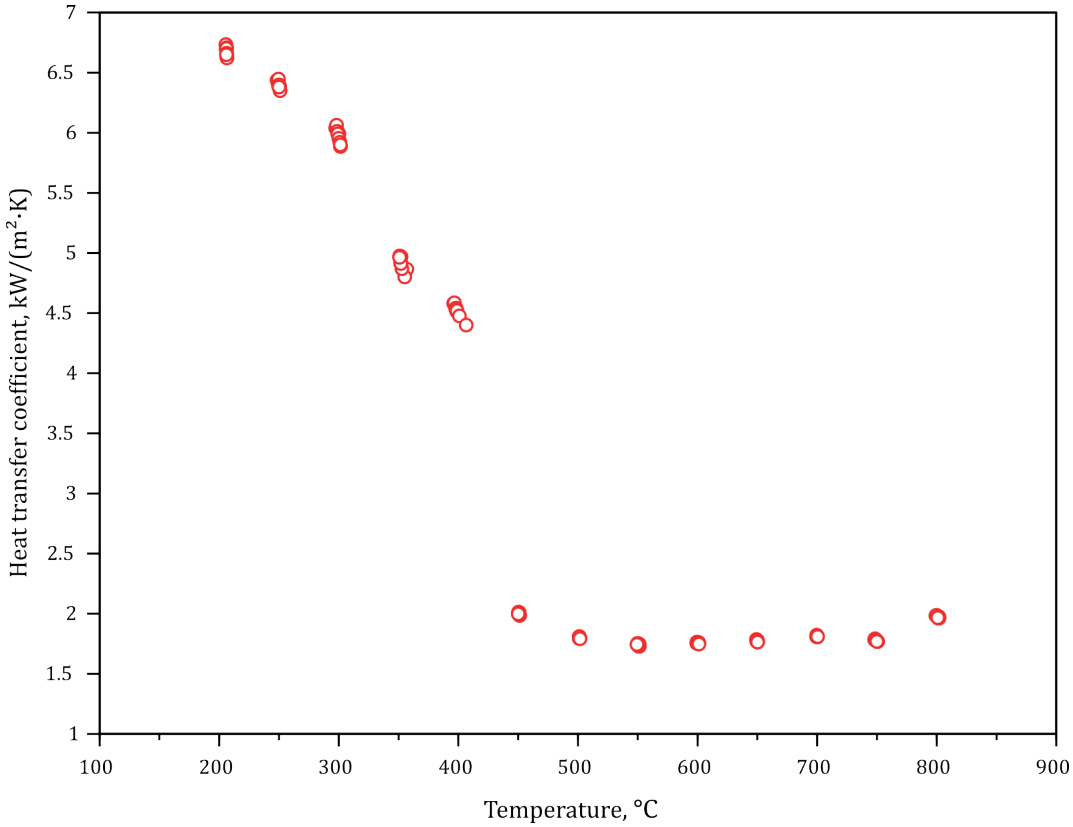


**Fig. 10.** Heat transfer coefficient as a function of temperature

Using the quantitative data from the power dissipated on the heating element, the heat transfer coefficient was calculated as a function of surface temperature from the equation (in connection with Figure 8):

$$\alpha = \left( \frac{Q_T}{T_D - T_m} \right) \tag{3}$$

The results of the calculations are presented in Figure 10. The results obtained are consistent with those obtained by other researchers [5]. The advantage of the presented research is that it provides results for the entire temperature range occurring in the isothermal quenching process for obtaining an ausferrite structure in ductile iron. The sharp observed change in heat generation (Fig. 9) and in the heat transfer coefficient (Fig. 10) within the 400–450°C temperature range is associated with the well-known effect of vapor-jacket formation effect. This layer prevents direct contact between the evaporating liquid and the metal surface. The described effect and the temperature at which this transition occurs were named after Leidenfrost, the author who described the phenomenon [20].

## 4. DISCUSSION OF RESULTS

The advantage of the proposed test method is that it provides results across the entire range of temperatures of isothermal quenching of ADI. The Leidenfrost temperature was determined, which for the analyzed parameters of water mist and the test sample was in the range of 400–450°C. The results obtained are consistent with those published in [5].

This study is not without its flaws. Namely, it is difficult to estimate or measure heat losses, i.e., the heat flux $Q_R$ flowing from the heating element to the environment by means other than through the test plate (Fig. 8). In the study the heat transfer coefficient was assessed on the basis of the power emitted by the heating element under conditions of stable recorded sample temperature. Under these conditions, most of the heat dissipated was related to the heating and evaporation of the sprayed water droplets. However, there were heat losses associated with the cooling of other components of the installation that were not exposed to the spray. These losses caused the results to be overestimated in relation to the actual value but do not affect the assessment of the Leidenfrost temperature. At this stage, the value of these losses in relation to the heat output was not quantitatively assessed.

## 5. SUMMARY

1. The results of the study indicate the potential for using water mist as a cooling medium in the processing of ADI cast iron as an alternative to molten salts.
2. The study showed that the heat transfer coefficient via spraying (1700–6700 W/(m²·K)) is significantly higher than that for a salt bath (550–1100 W/(m²·K)) [21], which is significant because, with proper control, a cooling profile can be achieved that is unattainable with conventional heat treatment using other cooling media.
3. The results of the study, covering such a wide measurement range provide a basis for developing a more comprehensive numerical model of heat treatment of ADI cast iron using water mist.

**REFERENCES**


[1] Stręk P. (2024). Theoretical possibilities of controlling the cooling rate in the heat treatment of cast iron with water mist. *Journal of Casting & Materials Engineering*, 8(4), 68–73. DOI: https://doi.org/10.7494/jcme.2024.8.4.68.

[2] Władysiak R., Kozuń A. & Pacyniak T. (2017). The effect of water mist cooling of casting die on the solidification, microstructure, and properties of AlSi20 alloy. *Archives of Metallurgy and Materials*, 62(1), 187–194. DOI: https://doi.org/10.1515/amm-2017-0026.

[3] Czekaj E., Kwak Z. & Garbacz-Klempka A. (2017). Comparison of impact of immersed and micro-jet cooling during quenching on microstructure and mechanical properties of hypoeutectic silumin AlSi7Mg0.3. *Metallurgy and Foundry Engineering*, 43(2), 153–168. DOI: https://doi.org/10.7494/mafe.2017.43.3.153.

[4] Mudawar I. & Valentine W.S. (1989). Determination of the local quench curve for spray-cooled metallic surfaces. *Journal of Heat Treating*, 7(2), 107–121. DOI: https://doi.org/10.1007/BF02833195.

[5] Flores T., Castillejos H. & Thomas B. (2017). Heat extraction and droplet impact regimes obtained with continuous casting air-mist nozzles. *AISTech 2017 Proceedings of the Iron & Steel Technology Conference. Vol. II*, Nashville, TN, USA, pp. 1751–1760.

[6] Tenzer F.M. (2020). *Heat transfer during transient spray cooling: An experimental and analytical study* [PhD thesis]. Fachbereich Maschinenbau der Technischen Universität Darmstadt, Darmstadt.

[7] Puschmann F., Schmidt J. & Specht E. (2000). Evaporation quenching with atomized sprays. *Proceedings of the 3rd European Thermal Science Conference*, Heidelberg, pp. 1071–1074.

[8] Sözbir N., Chang Y. & Yao S. (2003). Heat transfer of impacting water mist on high temperature metal surfaces. *Journal of Heat Transfer*, 125(1), 70–74. DOI: https://doi.org/10.1115/1.1527913.

[9] Jasiewicz E., Hadała B., Cebo-Rudnicka A., Malinowski Z. & Jasiewicz K. (2023). Comparison of the heat transfer efficiency of selected water cooling sytems. *SSRN Electronic Journal*. DOI: https://doi.org/10.2139/ssrn.4333923.

[10] Fang Y. Sabariman S. Specht E. (2016). Analytical Model for Describing Experimental Results on Parameters Influencing Heat transfer in Film Boiling with Spray Quenching. *Proceedings of 12th International Conference on Heat Transfer, Fluid Mechanics and Thermodynamics, Costa del Sol, Malaga, Spain.*

[11] Labergue A., Lemoine F., Aiguier T. & Gradeck M. (2014). Comparative study of the cooling of a hot temperature surface using spray and liquid jet. In: *15th International Heat Transfer Conference (IHTC-15), 2014. Kyoto, Japan*, pp. 2415–2429. DOI: https://doi.org/10.1615/IHTC15.evp.009287.

[12] Pohanka M. & Kotrbáček P. (2012). Design of Cooling Units for Heat Treatment. In: Czerwinski F. (Ed.), *Heat Treatment – Conventional and Novel Application.* DOI: https://doi.org/10.5772/50492.

[13] Van der Geld C.W.M., Passos J.C. & Leocadio H. (2019). Heat transfer coefficient during water jet cooling of high-temperature steel. In: *11th International Rolling Conference, (IRC 2019) São Paulo*, pp. 763–773. DOI: https://doi.org/10.5151/9785-9785-32400.

[14] Hadała B., Cebo-Rudnicka A. & Radziszewska A. (2022). Identification of the boundary condition of heat transfer during spray cooling process of the oxidized surface. *SSRN Electronic Journal*. DOI: https://doi.org/10.2139/ssrn.4167471.

[15] Fujimoto H., Hatta N., Asakawa H. & Hashimoto T. (1997). Predictable modeling of heat transfer coefficient between spraying water and a hot surface above the Leidenfrost temperature. *ISIJ International*, 37(5), 492–497. DOI: https://doi.org/10.2355/isijinternational.37.492.

[16] Cebo-Rudnicka A. (2011). *Wpływ warunków chłodzenia oraz przewodności cieplnej wybranych metali na współczynnik wymiany ciepła w procesie chłodzenia z natryskiem wodnym* [PhD thesis]. Kraków: Akademia Górniczo-Hutnicza

[17] Władysiak R. & Budzyński P. (2012). Structure of water mist stream and its impact on cooling efficiency of casting die. *Archives of Foundry Engineering*, 12(2), 251–260. DOI: https://doi.org/10.2478/v10266-012-0069-y.

[18] Chabičovský M., & Horský J. (2017). Factors influencing spray cooling of hot steel surfaces. In: *Metal 2017, Brno, Czech Republic*. Brno: Brno University of Technology, Faculty of Mechanical Engineering, pp. 77–82. URL: https://www.confer.cz/metal/2017/read/1345-factors-influencing-spray-cooling-of-hot-steel-surfaces.pdf.

[19] Baumeister K.J., Henry R.E. & Simon F.F. (1970). Role of the surface in the measurement of the Leidenfrost temperature. In: Bergles A.E. & Webb R.L. (Eds.), *Augmentation of Convective Heat and Mass Transfer. Papers presented at the Winter Annual Meeting of the American Society of Mechanical Engineers*, New York: American Society of Mechanical Engineers. Heat Transfer Division, pp. 91–101.

[20] Leidenfrost J.G. (1966). On the fixation of water in diverse fire. *International Journal of Heat and Mass Transfer*, 9(11), 1153–1166. DOI: https://doi.org/10.1016/0017-9310(66)90111-6.

[21] Myszka D. & Babul T. (2006). Obróbka cieplna żeliwa sferoidalnego w złożach fluidalnych. *Archiwum Odlewnictwa*, 6(20), 177–184.